33rd Annual International Conference of the IEEE EMBS
Boston, Massachusetts USA, August 30 - September 3, 2011

Fuzzy Approach toward Reducing False Positives in the Detection of Small Multiple Sclerosis Lesions in Magnetic Resonance Images

F. X. Aymerich, *Member, IEEE,* P. Sobrevilla, Senior *Member, IEEE*, E. Montseny, *Member, IEEE,* and A. Rovira

Abstract— **The large number of false positives that result when automatic algorithms are considered for segmenting small multiple sclerosis lesions in magnetic resonance imaging hampers the posterior evaluation of lesion load. To address this problem we propose a fuzzy system which can improve the differentiation between true and false positive detections in proton density- and T2-weighted images. On the basis of an earlier work, which was focused on the detection of hyperintense regions in MR brain images, the system here presented introduces fuzzy restrictions derived from the regional analysis of the main features in such regions. Results show a reduction to a 3.6% in the number of false detections while preserving most of the true detections obtained using previous algorithm.**

I. INTRODUCTION

THE presence of multiple sclerosis (MS) lesions can be visualized in brain magnetic resonance (MR) images by alterations in the gray-level intensity of the regions wherein this pathology is present. Nevertheless a direct correspondence between the alterations of gray level and the presence of pathology can not be established, because there are other areas in the images that also show hyper or hypointensity in relation to its local surrounding, what suppose a trouble for designing automatic detection and segmentation algorithms.

Although different weighted images can be used for visualizing MS lesions, dual acquisition of proton density (PD-) and T2-weighted images are the most commonly used for evaluating its lesion volume [1].

The detection of regions corresponding to MS lesions in MR images is an arduous and complex task. This is due to detection of lesions involves the analysis of several images with different anatomical features, and presents a high dependence of the contrast-to-noise ratio in the images. Moreover, MS lesions are inherently fuzzy with an uncertainty component in their boundary definition [2].

Although some authors, [3]-[7], have developed algorithms for detecting MS lesions, the obtaining of full automatic solutions free of false positives is a difficult task. Most false positives are related to the presence of small regions in the images and the difficulty in its differentiation from small MS lesions. To overcome this problem, these algorithms require the elimination of false detections manually or the prior exclusion of regions whose size is below a preset minimum.

The presence of noise, inhomogeneities, and other characteristic factors of MR images, make difficult for an automatic MS detection algorithm get rid of false positives and recognize lesions following the expert way of work. An added difficulty factor that has to be taken into consideration for avoiding false positives in the case of small lesions is the large proportion of border pixels with respect to pixels within the lesion.

The algorithm here presented introduces different strategies to filter out false detections, and is focused on the differentiation between small MS lesions and false detections obtained using our previous fuzzy detection approach [8]. With this aim the algorithm will be fed on location, size, and other regional characteristics of the detections that were not considered at previous work. The rest of the paper is structured as follows: Section II includes a short description of the previously developed algorithm [8], which is used as starting point to this work. The proposed strategies considered for reducing false detections are introduced at section III. Finally, at section IV, we present some results and the conclusions of the proposed work.

II. INITIAL DETECTION OF SMALL MS LESIONS

In a previous work, [8], we presented a fuzzy-based algorithm to detect small hyperintense regions in PD- and T2-weighted MR images addressed to the detection of MS lesions. We considered eight PD- and eight T2-weighted brain axial images acquired in a 1.5T Magnetom Vision MR System (Siemens, Erlangen, Germany) using a dual turbo spin-echo sequence (TR/TE/NEX/Matrix/FOV/Thickness: 3000ms/12-80ms/1/256x256/250mm/3mm). These images corresponded to slices associated with four representative brain locations showing different levels of lesion load.

Based on the protocol followed by the experts for detecting MS lesions in the considered images, small MS

This work has been partially supported by the Spanish CICYT Project TIN2007-68063

F. X. Aymerich is with the Magnetic Resonance Unit - IDI, Vall Hebron University Hospital, E-08035 Barcelona, Spain (phone: +34934289406; fax: +34934286059; e-mail: xavier.aymerich@idi-cat.org) and with the Computational Engineering and Industrial Systems (ESAII) Department, Technical University of Catalonia, E-08034 Barcelona, Spain (e-mail: xavier.aymerich@upc.edu).

P. Sobrevilla is with the Applied Mathematics II Department, Technical University of Catalonia, E-08034 Barcelona, Spain (e-mail: pilar.sobrevilla@upc.edu).

E. Montseny is with the ESAII Department, Technical University of Catalonia, E-08034 Barcelona, Spain (e-mail: eduard.montseny@upc.edu).

A. Rovira is with the MR Unit - IDI, Vall Hebron University Hospital, E-08035 Barcelona, Spain (e-mail: alex.rovira@idi-cat.org)

lesions were defined as hyperintense regions located in the encephalic parenchyma, with a minimum size of three pixels, and fully contained within a 5x5 raster window.

The *hyperintensity characterization and evaluation* was carried out considering a 9x9 raster window centered on the pixels of the MS small lesions marked by neuroradiologists, and considering that: 1) The gray level of hyperintense pixels is high enough; 2) A pixel has hyperintense behavior if its gray-level is sufficiently distinguishable from the gray levels of two adjacent pixels for a sufficiently large number of main radii within the 9x9 window; and 3) A region can be associated with MS lesion if its pixels present hyperintense behavior at both PD- and T2-weighted images.

Following previous considerations, the fuzzy sets that evaluate the hyperintensity of pixels at both weighted images, $\mu_{H,P}$ (P=PD, T2), were obtained aggregating the hyperintensity membership functions at the eight main radii, $\mu_P^{r_i}$ ($1 \le i \le 8$, P=PD, T2), by means of Ordered Weighted Averaging (OWA) operators [9]. The selection of the weighting vectors was accomplished applying a *Mamdani type Fuzzy Rule-Based System* (MFRBS).

$$\mu_{H,P}(p_{ij}) = f_{w_P}(\mu_P^{r_1}(p_{ij}),..., \mu_P^{r_8}(p_{ij})) = (0,0,0,1,0,0,0,0) \cdot (\mu_P^{r_{\sigma(1)}}(p_{ij}),..., \mu_P^{r_{\sigma(8)}}(p_{ij}))^T . \quad (1)$$

where $\mu_P^{r_{\sigma(i)}}(p_{ij})$ is the i-th largest of the $\mu_P^{r_i}(p_{ij})$.

After implementing a MFRBS at which the more usual "logical and" operators were considered, Previous membership functions were aggregated for obtaining the hyperintensity membership function μ_H as follows.

$$\mu_H(p_{ij}) = \sqrt{\mu_{H,PD}(p_{ij})\mu_{H,T2}(p_{ij})} . \quad (2)$$

Finally, the hyperintense regions associated with small MS lesions were obtained by applying a 0.5-cut to the hyperintense fuzzy set, and performing an 8-connectivity analysis of the detected pixels in each image.

III. Reduction of False Detections

With the aim of filtering out false detections obtained by previous algorithm, while preserving its sensitivity, we introduce location, size, and other regional characteristics of small lesions that were not considered for obtaining the membership function μ_H of (2). The design dataset here considered is the defined at the beginning of section II.

A. Location restrictions

Whilst the definition of small MS lesion given in previous section restricts its location to the encephalic parenchyma, at previous algorithm the whole intracranial region was considered. So, besides the encephalic parenchyma, cerebrospinal fluid regions (CSF), such as the ventricular region or the brain sulci were considered. Because of in PD-weighted images some pixels belonging to thin regions or to areas within wider fluid regions may show hyperintensity, and so turn out into false positives, the first constraint was addressed to ruling out these pixels.

The location restriction here considered is based on the use of the *Confidence Fluid Regions* (CFR) fuzzy set, μ_{CFR}, introduced in [10], which provides the degree to which a CSF pixel has low possibility of misclassification as MS lesion pixel. So we draw upon for removing this kind of false detections. Then, if I_{CFR} is the binary image obtained applying a 0.55-cut to μ_{CFR}, and $\delta_{C2}(I_{CFR})$ is the image obtained applying to I_{CFR} morphological dilation with a 2 pixel radius circular structuring element (C2), we define the membership function:

$$\varphi_H(p_{ij}) = \begin{cases} 0 & \text{if } \delta_{C2}(I_{CFR})(i,j) > 0 \\ \mu_H(p_{ij}) & \text{otherwise} \end{cases} . \quad (3)$$

Although φ_H will allow us to eliminate pixels located within or close to confidence fluid regions, it can also remove some true detections. With the aim of avoiding this drawback the hyperintensity values of true detection pixels are modified considering a dilation of image I_φ, subject to image I_H, and the element C2 ($\delta(I_\varphi, I_H, C2)$), where I_H and I_φ are the binary images obtained applying a 0.5-cut to μ_H and φ_H. So, once the location restriction is considered, the degree to which a pixel is hyperintense is given by:

$$\psi_H(p_{ij}) = \begin{cases} \mu_H(p_{ij}) & \text{if } \delta(I_\varphi, I_H, C2)(i,j) > 0 \\ \varphi_H(p_{ij}) & \text{otherwise} \end{cases} . \quad (4)$$

B. Size restrictions

With the aim of guarantee that the size of the detected hyperintense regions fit size characteristics of small MS lesions, it is necessary to take into account that the presence of noise and inhomogeneities may cut down the hyperintensity values of some pixels. This reduction will affect the actual size of the detected regions that will become false detections.

To eliminate false detections due to the above problem we carry out a local neighborhood-based review process of those pixels p_{ij} such that $\psi(p_{ij})=\alpha$, and $0.1 \le \alpha \le 0.5$. To do it, for each α, if $\psi(p_{ij})>\alpha$ and more than 2 pixels within its 8-neighborhood of p_{ij} have hyperintensity degree greater than 0.5 ($n_8(p_{ij})>2$), we assign p_{ij} the value $v_H(p_{ij})$ given by $\max\left\{\psi_H(p_{ij}), \frac{\psi_H(p_{i-1,j})+\psi_H(p_{i+1,j})}{2}, \frac{\psi_H(p_{ij-1})+\psi_H(p_{ij+1})}{2}\right\}$. So we obtained the improved hyperintensity membership function:

$$\chi_H(p_{ij}) = \begin{cases} v_H(p_{ij}) & \text{if } \psi_H(p_{ij}) > \alpha \text{ and } n_8(p_{ij}) > 2 \\ \psi_H(p_{ij}) & \text{otherwise} \end{cases} . \quad (5)$$

Then, to filter out regions that do not fit size restrictions

of small MS lesion we analyze the 8-connectivity and introduce the function $sv_8(p_{ij})$ that equals zero if $\chi_H(p_{ij})>0.5$ *and the maximum of the horizontal or vertical distances between the locations of the pixels 8-connected with the* p_{ij} *is greater than 4; or* $\chi_H(p_{ij})>0.5$ *and* p_{ij} *belongs to a 8-connected region with less than 3 pixels*. Considering this function the degree to which a pixel is hyperintense is given by:

$$\vartheta_H(p_{ij}) = \begin{cases} \min(0.3, \chi_H(p_{ij})/2) & \text{if } sv_8(p_{ij}) = 0 \\ \chi_H(p_{ij}) & \text{otherwise} \end{cases}. \quad (6)$$

C. Restrictions based on gray level

As previously said, small MS lesions are regions constituted by pixels showing hyperintensity in PD- and T2-weighted images (I_{PD} and I_{T2}). So, the proposal here considered consists on evaluating the gray-level values inside and outside detected regions considering the product images $I_{\Pr od}(p_{ij}) = \sqrt{I_{PD}(p_{ij}) I_{T2}(p_{ij})}$.

Hyperintense regions no adjacent to other hyperintense regions should show greater gray level inside than in its outer proximity. So, to distinguish among pixels within ($I(R_k)$) and outside ($O(R_k)$) detected regions R_k, we study the mean and standard deviation of pixels within the regions ($m(R_k)$, $\sigma(R_k)$). Moreover, to locate the pixels in the outer proximity of detected regions, $op(R_k)$, we analyze their external morphological gradients $mg(op(R_k))$. Then, if all pixels in $op(R_k)$ show a gray level lower than $m(R_k)$-$\beta\sigma(R_k)$, the region R_k will be considered as actually hyperintense.

To implement previous restriction we introduce the boolean function $glf(p_{ij})$ that equals 0 if p_{ij} belongs to R_k and $\max(mg(op(R_k)))>m(R_k)$-$\beta\sigma(R_k)$, and equals 1 in other case. Considering this function the degree to which a pixel is hyperintense is given by:

$$\zeta_H(p_{ij}) = \begin{cases} \vartheta_H(p_{ij})/2 & \text{if } glf(p_{ij}) = 0 \\ \vartheta_H(p_{ij}) & \text{otherwise} \end{cases}. \quad (7)$$

D. Restrictions based on other regional features

The last strategy for reducing false detections is based on the analysis of 22 regional features that are studied individually and by pairs in order to obtain the best combinations of features that allow reducing false positives but preserving the sensitivity.

After selecting the features that graphically show a better discrimination between true and false detections, we applied the Nelder and Mead optimization algorithm [11] for getting the parameters, in function of individual or paired analysis, that offer the optimum trade-off between sensitivity and false positives. In order to refine the optimization we repeat the analysis by including and excluding features until getting a subset of features and parameters that show stability in the improvement of the trade-off value.

Finally, the eight out of the twenty-two selected features were: Mean Hyperintensity membership degree of the pixels in the region ($M\zeta_H$); Ratio between Mean Hyperintensity Memberships in the outer ring and the interior region ($RM\zeta_H$); Mean Gray-Level of pixels inside (*MGLP*), and on the outer Ring (*MGLPR*) of a region in the product image; Ratio between the Mean Gray-Levels in the outer ring and the interior region in the Product image (*RMGLP*); Ratio of maxima Distances in x and y directions (*RDxy*), Filling Factor, (*FF*), or proportion of pixels in a region regarding the product of maximum distances in the x and y directions in the region; and Compactness Factor, (*CF*), or proportion between the number of pixels in a region and the maximum distance in the x and y directions in the region.

Then, using these features and the parameters selected by the optimization algorithm we introduce some regional restrictions. To do it, if $frf(p_{ij})$ equals 1 if $\zeta_H(p_{ij})>0.5$ and p_{ij} satisfies at least one of the restrictions defined from the selected features and parameters, and equals 0 in other case, the final hyperintensity membership function is given by:

$$\eta_H(p_{ij}) = \begin{cases} \zeta_H(p_{ij})/2 & \text{if } frf(p_{ij}) = 1 \\ \zeta_H(p_{ij}) & \text{otherwise} \end{cases}. \quad (8)$$

IV. Results and Conclusions

The proposed algorithm was evaluated on 184 PD- and T2-weighted images, corresponding to four patients with clinically definite MS, in which lesions were delineated by a trained operator and validated by a neuroradiologist. For getting the binary images resulting from the previous filtering process, we a 0.5-cut to the images $I'_H(i,j) \equiv \eta_H(p_{ij})$ for obtaining the images I_{DH} containing the detections associated with the presence of hyperintensity.

To carry out the performance analysis of previous detection algorithm and the filtering approach here presented we considered following parameters: *True Positives*, *TP*, or number of regions marked up as small lesions (*sl*) by the experts and detected by the algorithm; *False Negatives*, *FN*, or number of regions marked up as *sl* by the experts but undetected by the algorithm; and *False Positives*, *FP*, or number of regions detected as *sl* by the algorithm but unmarked up by the experts.

Using previous parameters two regional quality indexes were considered: *False Negatives*; and *Sensitivity in the detection of MS small lesions*, defined as *S=TP/(TP+FN)*.

Before obtaining the results the values of the parameters α and β, considered for defining χ_H (in (5)) and ζ_H (in (7)) were obtained. The selection of α was based on the analysis of χ_H looking for a trade-off between true and false positives considering values of α within the interval [0.1, 0.5]. After this analysis the chosen value was α=0.3.

For selecting the value of β we considered that a negative value of this parameter would be a consequence of the hypothesis that gray level values outside a region should be

lower than the mean value inside the region. So after analyzing the results obtained for the values of β within the interval [-1, 1.4], the optimum value was β=0.2.

Regarding the parameter considered in section III.D, the Nelder and Mead algorithm allowed us to introduce the following restrictions: a) $M\zeta_H$<0.668; b) $RM\zeta_H$>0.359; c) *MGLP*>170.75; d) *MGLPR*>97,004; e) *RMGLP*>1.826($M\zeta_H$-0.314); f) *RDxy*<0.230; g) *RDxy*>3.078; h) *FF*<0.396; i) *FC*<0.582.

Table I shows the mean values of *S* and *FP* obtained by the initial detection proposal (row two), and after introducing the filtering restrictions (row three). In the case of the initial detection algorithm, while the quality values obtained for the design data images were *S*=1.0 and *FP*=243.62, when this algorithm is applied to the test images (row two) it can be appreciated that sensitivity is almost the same and the number of false detections, although has reduced, remains too high.

By comparing the above results with those obtained after introducing the filtering restrictions (row three of table I), it can be appreciated that the introduction of the restrictions allows reducing the number of false detections to a 3.6% of the initial value (column three). This reduction makes up the decrease in the sensitivity, which still remains high enough. These results are also shown in Fig. 1, in which magenta regions correspond to detected small MS lesions for initial proposal, (c), and after applying the proposed algorithm, (d).

TABLE I
SUMMARY OF RESULTS FOR IMAGES IN THE TEST SET

Analysis	*S*	*FP*
Initial Detection	0.995	174.21
Improved algorithm	0.760	6.27

S: Sensitivity; FP: False positives.

As conclusion, in this paper we have presented an algorithm that introduces different strategies to filter false detections in MR images addressed to the detection of small hyperintense regions associated with MS lesions. We have applied this approach to improve the results obtained in a previous fuzzy algorithm [8] for detecting small MS lesions.

The proposed strategies have been focused on introducing regional restrictions, which the initial algorithm did not include, in order to obtain an optimized membership function. As results show, the new membership function allows reducing the number of false detections to acceptable levels, but maintaining high enough detection levels.

The obtained results suggest that the proposed algorithm can be used to complement the existing small MS lesions detection algorithm, or as starting point in the design of a new automatic MS lesion segmentation algorithm.

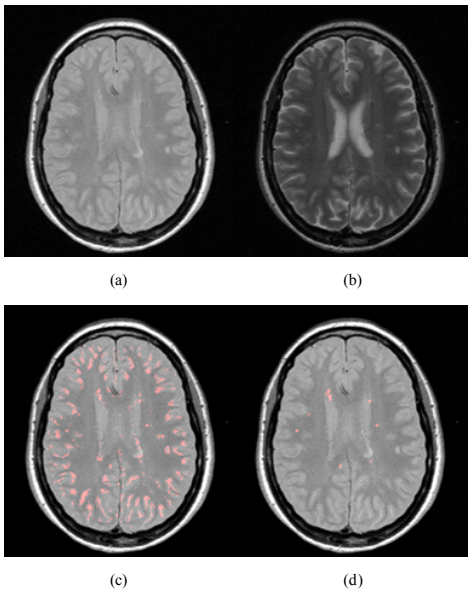

Fig. 1. Example of detections obtained for the PD- and T2 -weighted images (a) and (b). Magenta regions in images (c) and (d) correspond to the detections obtained by the initial proposal and after applying the proposed algorithm to reduce false detections.

REFERENCES

[1] P. A. Narayana, M. Metha and J. Wolinsky, "Magnetic resonance in multiple sclerosis," in *Recent Advances in MR Imaging and Spectroscopy*, N. R. Jagannathan, Ed. New Delhi: Jaypee Brothers Medical Publishers Ltd, 2005, pp. 154-185.

[2] D. H. Miller, R. I. Grossman, S. C. Reingold and H. F. McFarland, "The role of MR techniques in understanding and managing multiple sclerosis," *Brain*, vol. 121, no. 1, pp. 3-24, Jan. 1998.

[3] A. Akselrod-Ballin, M. Galun et al.., "Automatic segmentation and classification of multiple sclerosis in multichannel MRI," *IEEE Trans. Biomed. Eng.*, vol. 56, no. 10, pp. 2461-2469, Oct. 2009.

[4] B. R. Sajja, S. Datta et al., "Unified approach for multiple sclerosis lesion segmentation on brain MRI," *Ann. Biomed. Eng.*, vol. 34, no. 1, pp. 142-151, Jan. 2006.

[5] F. Admiraal-Behloul, D. M. J. van den Heuvel et al., "Fully automatic segmentation of white matter hyperintensities in MR images of the elderly," *Neuroimage*, vol. 28, no. 3, pp. 607-617, Nov. 2005.

[6] K. Van Leemput, F. Maes, D. Vandermeulen, A. Colchester and P. Suetens, "Automated segmentation of multiple sclerosis lesions by model outlier detection," *IEEE Trans. Med. Imaging*, vol. 20, no. 8, pp. 677-688, Aug. 2001.

[7] J. K. Udupa, L. Wei et al., "Multiple sclerosis lesion quantification using fuzzy-connectedness principles," *IEEE Trans. Med. Imaging*, vol. 16, no. 5, pp. 598-609, Oct. 1997.

[8] F. X. Aymerich, E. Montseny, P. Sobrevilla and A. Rovira, "Detection of hyperintense regions on MR brain images using a Mamdani type fuzzy rule-based system. Application to the detection of small multiple sclerosis lesions," in *2011 IEEE Int. Conf. on Fuzzy Systems*, accepted for publication.

[9] R. R Yager., "Families of OWA Operators," *Fuzzy Sets and Systems*, vol. 59, pp. 125-148, 1993

[10] F. X. Aymerich, E. Montseny, P. Sobrevilla and A. Rovira, "A fuzzy regional-based approach for detecting cerebrospinal fluid regions in presence of multiple sclerosis lesions." *2010 IPMU Conf.*, in *CCIS,* vol. 81, part II, pp. 552-561 Springer-Verlag: Berlin, 2010.

[11] J. A. Nelder and R. Mead, "A simplex method for function minimization," *Comp. Journal*, vol. 7, no. 4, pp. 308-313, Jan. 1965.